Marine phytoplankton community structure of the waters of the Argentine Islands (2019-2021)

Andrii Zotov[1,2*], Mariia Pavlovska[1], Artem Dzhulai[1], Evhen Dykyi[1]

[1]*National Antarctic Scientific Center, Ministry of Education and Science of Ukraine, Shevchenko Blvd. 16, 01601, Kyiv, Ukraine*
[2]*Institute of Marine Biology, National Academy of Sciences of Ukraine, Pushkinska St. 37, 65125, Odesa, Ukraine*

Abstract

The variability of phytoplankton community structure was analyzed in the waters of the Argentine Islands in late summer period of 2019, 2020 and 2021, as well as from February 2020 to February 2021. Biodiversity (121 taxa) and phytoplankton structure of the Argentine Islands waters corresponded to earlier studies. The late summer succession in 2019 and 2020 and 2021 was found typical for the waters of the Argentine Islands. Representatives of *Bacillariophyceae* completely dominated the studied community. Biomass variability was largely determined by large centric diatoms with low specific surface (S/W) values ranging from 70 to 300 $m^2 \cdot kg^{-1}$. Higher values of phytoplankton development metrics and a more noticeable presence of haptophyte, cryptophyte and diatom groups with S/W values larger than 700 $m^2 \cdot kg^{-1}$ differed 2019 from 2020 and 2021. Lower development metrics and simplified taxonomic structure of phytoplankton were recorded in 2020 – 2021. The decrease in the specific surface of the groups in the late summer periods of 2020 and 2021 was caused both by a decrease in the relative contributions of small-celled Coccolithophyceae and Cryptophyceae and by a general decrease in S/W of these taxa. Characteristic annual phytoplankton development patterns were revealed. The spring phytoplankton development was formed by high abundance of *Fragilariopsis* with a predominant contribution to the biomass of large centric diatoms. At the beginning of austral summer, the role of flagellates from the genera *Cryptomonas* (*Cryptophyta*) and *Pyramimonas* (*Chlorophyta*), as well as small flagellates, increased. The late austral summer period was characterized by the dominance of large centric diatoms with a significant presence of small flagellates and a periodic increase in the contribution of *Fragilariopsis*. The spring-summer succession had common features with the development of phytoplankton in the more northern regions of the Western Antarctic Peninsula (Palmer station), while the late summer phase – with the more southern Rothera station.

Key words: phytoplankton, Western Antarctic Peninsula (WAP), Argentine Islands, succession, monitoring, biomass, specific surface.

DOI: 10.5817/CPR2024-2-16

Received October 10, 2024, *accepted* January 14, 2025.
[*]Corresponding author: A. Zotov <zotovab@ukr.net>

Introduction

Antarctic coastal areas are characterized by high primary productivity (Arrigo et al. 2017). In the waters of the Western Antarctic Peninsula (WAP), it is close to other areas of the continental shelf of Antarctica and is about 182 $gC \cdot m^{-2}$ per year (Arrigo et al. 2008), which is about four times lower than in the most productive coastal regions of the World Ocean (Vernet and Smith 2007, Nardelli et al. 2023). This difference is naturally determined by the temperature, light and ice cover, that limit the level of WAP phytoplankton development, especially in the autumn-winter period. The main phytoplankton production is formed during spring-summer development, when chlorophyll concentrations in WAP waters can exceed 20 $\mu g \cdot l^{-1}$ (Vernet et al. 2008, Ducklow et al. 2013, Kim et al. 2018). Phytoplankton productivity and structure affects the development of all subsequent components of the Antarctic food chain (Moline et al. 2004, Saba et al. 2014, van Leeuwe et al. 2020). In addition, microalgae play an important role in the response of the Antarctic ecosystem to climate change through the absorption of CO_2 (Legge et al. 2017) and the production of climate-active gases (Stefels et al. 2018, Webb et al. 2019, Hughes et al. 2009).

The WAP has experienced significant and rapid climatic changes in recent decades (Meredith and King 2005, Stammerjohn et al. 2008). During the second half of the twentieth century, WAP warming rates were the largest in the Southern Hemisphere, leading to an increase in ocean surface temperature of more than 1°C (Meredith and King 2005, Turner et al. 2005). These processes have continued after a certain period of stabilization (Turner et al. 2016). As of 2016, 90% of sea glaciers have retreated, and the annual sea ice season has shortened by >92 days since 1979 (Stammerjohn et al. 2012, Cook et al. 2016). Further warming in Western Antarctica is predicted during the 21st century (Meijers 2014).

Biological systems of Antarctic coastal areas are extremely sensitive to climate change due to the adaptation of marine organisms to a limited range of environmental conditions at the level of diversity, physiology, and involvement in marine biogeochemical cycles (Steiner and Stefels 2017). The close relationship between environmental conditions and phytoplankton components (community structure) suggests that continued warming in the WAP will affect the seasonal dynamics of phytoplankton and subsequently the seasonal dynamics of the food web (Nardelli et al. 2023). It is expected that ocean warming, sea ice and glacier retreat, causing increased spatial distribution of low-salinity surface waters, will lead to higher abundance of small-celled phytoplankton along the WAP (Moline et al. 2004). This will have important implications for food web structure and for the efficiency of trophic energy transfer (Sailley et al. 2013). So far, there is a trend towards a decrease in the summer phytoplankton biomass and in the size of the cells forming it in the northern WAP (Montes-Hugo et al. 2008, 2009; Nardelli et al. 2023). It is assumed that such morphological rearrangement is caused by an increase in the number of small-celled cryptophytes in coastal regions (Moline et al. 2004, Mendes et al. 2013, 2018; Schofield et al. 2017), associated with broader adaptation of cryptophytes to light conditions (Kaňa et al. al. 2012, Nardelli et al. 2023). In addition to cryptophytes, the abundance of other flagellates, such as haptophytes (Arrigo et al. 2017, Stefels et al. 2018), prasinophytes and chlorophytes (van Leeuwe et al. 2020), is predicted to increase. Expected near-future conditions with a more dynamic ice cover may result in increased primary production of particular species, as well as in overall algal biomass, with more scattered

wind-mixed summer blooms (van Leeuwe et al. 2020).

Phytoplankton responses to climate change are difficult to model and predict, as the studies on its structural and functional reorganization in response to the environmental factors are scarce. Meanwhile, the model predictions available to date cover large planetary scales (Henson et al. 2016). Decades of observations are required for the reliable regional modelling of the climate change impact, which is of utmost importance for the functioning of Antarctic ecosystems (van Leeuwe et al. 2020). Thus, phytoplankton monitoring is essential for the analysis of complex ecosystem seasonal responses and general trends (Deppeler and Davidson 2017, Henley et al. 2019). Palmer (Anvers Island) and Rothera stations (Adelaide Island) are the main locations of the WAP, where systematic studies of phytoplankton are carried out (van Leeuwe et al. 2020, Nardelli et al. 2023). Vernadsky station (Argentine Islands), where phytoplankton monitoring studies have also been conducted since 2002 (Seregin et al. 2005, Kuzmenko and Ignatiev 2007), is located between them, 50 km to the southwest of the Palmer station and 200 km to the northeast of the Rothera station. The fastest warming rates for WAP were recorded in the waters of the Argentine Islands (Khrystiuk et al. 2022), which make it a particularly relevant polygon for monitoring of phytoplankton, as the first responders to climate change. Thus, the purpose of the present study is to analyze the variability of phytoplankton community structure in the Argentine Islands' waters in 2019-2021 and to define the trends of its dynamics.

Material and Methods

Study site

Research was conducted during the summer seasons of the 24th, 25th, and 26th Ukrainian Antarctic expeditions, from February to April 2019, 2020, and 2021. Samples were also collected during the period of April 2020 – February 2021. In 2019 and 2020, samples were taken at 6 stations in the waters of the Argentine Islands archipelago (Fig. 1) (Supplementary, Table 1). The analysis of the results obtained in 2019-2020 showed a stable lack of statistically significant difference between the data obtained from some stations. Thus, the marine monitoring scheme was optimized in 2021 and sampling was carried out at three stations (1, 3 and 5) during the seasonal expedition, and at station 3 during the annual monitoring (April 2020 – February 2021) (Fig. 1.).

Sampling

Sampling was performed weekly during the seasonal expeditions of 2019, 2020 and 2021 and once every two weeks during the 2020-2021 annual monitoring. The vertical profile of salinity, temperature, fluorescence, and oxygen concentration was recorded with the hydrochemical probe (Rbr Concerto, Canada) at each sampling event. Water samples for phytoplankton quantitative analysis were taken with a 5-liter Niskin bottle at the surface (1 m) and in the deep fluorescence maximum (DCM) layer. Qualitative phytoplankton samples were taken at each of the monitoring stations using a plankton net with a mesh size of 5 μm. Quantitative analysis was per-

formed for 177 phytoplankton samples, while 258 samples were analyzed for the concentration of chlorophyll *a* and pheophytin (for the method, *see* below).

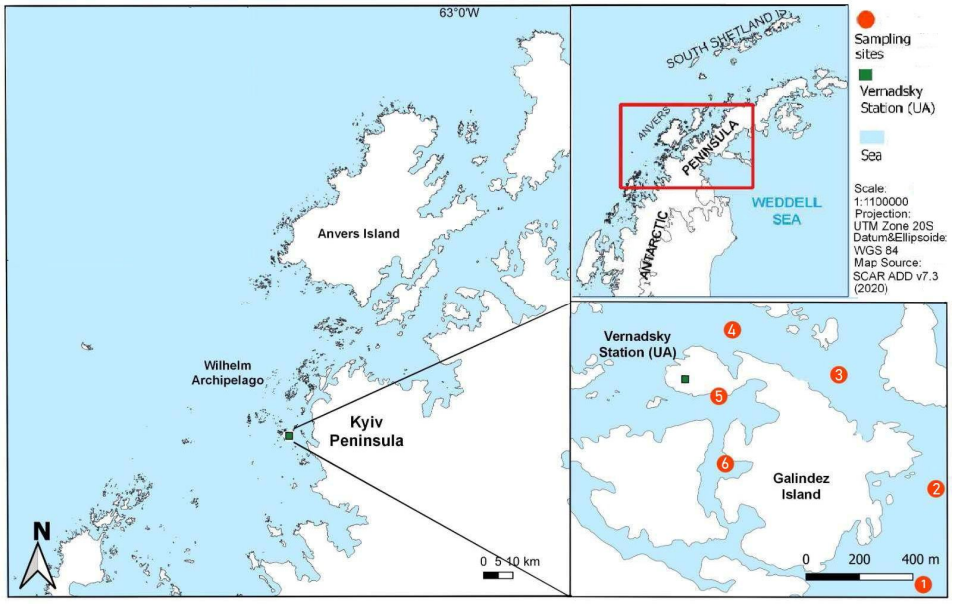

Fig. 1. Marine monitoring stations in the waters of the Argentine Islands archipelago, WAP.

Sample preparation and counting

Quantitative phytoplankton samples with a volume of up to 5 l were concentrated by reverse filtration through nitrocellulose filters with a pore diameter of 1.02 μm (Millipore) to a volume of 30-50 ml. Concentrated samples were fixed with a formaldehyde acidified with acetic acid to a final concentration of 4% formalin in the sample. If necessary, the samples were concentrated again by slow decantation to a volume of 10-15 ml before counting phytoplankton taxons. Quantitative and taxonomic processing of phytoplankton samples was carried out under a Zeiss Primo Star light microscope with magnifications of 400 – 1000. Cell counting was carried out in two replicates in a Najotta chamber with a volume of 0.05 ml. A Sedgwick-Raffer chamber with a volume of 1 ml was used for additional counting of large cells. Wet biomass was calculated by geometric similarity of the cells' shape to the corresponding geometric shapes and assuming that the density of cells is equal to 1. Metrics of surface area (S), surface index (IS) and specific surface (S/W) for different levels of phytoplankton organization were calculated based on Minicheva et al. (2003). The taxonomy was aligned with The World Register of Marine Species (WoRMS).

Chlorophyll *a* samples were collected by vacuum filtration (Combisart.jet Sartorius) through nitrocellulose filters with a pore diameter of 0.45 μm (Millipore) in duplicate for each station, followed by treatment of the filters with hot ethanol (90%, 78ºC) for pigments' extraction and subsequent centrifugation at 3000 rpm. Pigments' concentration was measured us-

ing Hach Lange DR3900 spectrophotometer. A solution of 0.3 ml hydrochloric acid and 100 ml ethanol was used to acidify the samples during the measurement.

Data analysis

The data was normalized via log-transformation. Fisher's least significant difference (LSD) with a 95.0% confidence level was used to detect a statistically significant difference between the means. Prism 10.1.1 (GraphPad Software) was used to create figures.

Results

Taxonomic composition and structure of phytoplankton

Representatives of 121 species and infraspecific taxa of unicellular algae, belonging to 12 taxonomic classes, were found in the Argentine Islands waters (Table 1; Fig. 2). Additionally, 30 taxa were encountered sporadically. They require further identification, which in most cases involves using molecular biology methods.

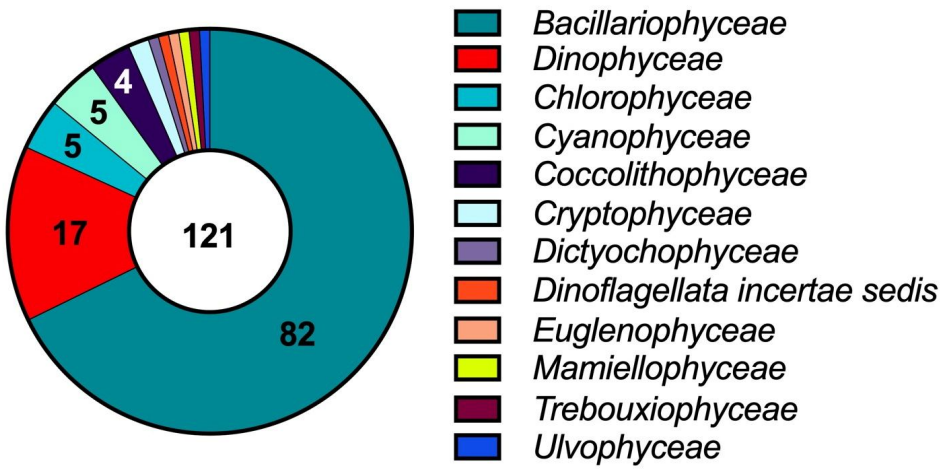

Fig. 2. Taxonomic distribution of the Argentine Islands phytoplankton at the class level based on the species number (February-April 2019, 2020 and 2021).

The highest species richness was found for the *Bacillariophyceae* class, which covered 68% of unicellular algae taxa (Fig. 2). *Dinophyceae* made up 14% of the total species number, and representatives of *Chlorophyceae* and *Cyanophyceae* – 4% each. The other taxonomic groups' contribution to the phytoplankton diversity did not exceed 3% (Fig. 2).

Species	2019	2020	2021	N_{total}, $10^6 \cdot m^{-3}$	B_{total}, $mg \cdot m^{-3}$
Bacillariophyceae					
Achnanthes antarctica Perag., 1921	+			1.73	5.68
Achnanthes brevipes C.Agardh, 1824	+	+		2.54	9.19
Achnanthes longipes C.Agardh, 1824			+	0.01	0.07
Actinocyclus octonarius var. octonarius Ehrenberg, 1837			+	0.01	0.06
Amphiprora kjellmanii var. kjellmanii Cleve in Cleve & Grunow, 1880	+	+	+	0.75	36.34
Amphiprora paludosa f. hyperborea Grunow in Cleve & Grunow, 1880	+			0.48	4.26
Amphora ovalis (Kützing) Kützing, 1844	+			0.98	11.66
Amphora veneta f. veneta Kützing, 1844	+	+	+	1.25	3.70
Berkeleya antarctica Grunow 1880	+	+	+	1.07	0.60
Cerataulina bergonii Ostenfeld, 1903		+		0.11	1.91
Ceratoneis closterium Ehrenberg, 1839	+	+	+	97.25	12.19
Ceratoneis fasciola Ehrenberg, 1839			+	0.00	0.06
Chaetoceros compressus Lauder, 1864	+	+	+	**714.35**	**448.70**
Chaetoceros neogracilis VanLand., 1968		+	+	0.31	0.15
Chaetoceros socialis H.S.Lauder, 1864		+		1.25	0.59
Chaetoceros sp.	+	+	+	5.46	10.08
Chaetoceros tortissimus Gran, 1900		+		0.70	0.52
Charcotiella irregularis (Perag.) S.Blanco & C.E.Wetzel, 2016	+			0.06	19.55
Cocconeis adeliae E. Manguin, 1960	+		+	0.50	38.49
Cocconeis costata var. antarctica Manguin, 1960	+	+	+	12.91	120.27
Cocconeis infirmata Manguin, 1957	+			0.65	4.75
Cocconeis sp.	+	+	+	0.10	4.18
Corethron criophilum Castracane, 1886	+	+	+	176.74	**8890.13**
Corethron inerme Karsten, 1905	+	+	+	7.18	**2142.0**
Coscinodiscus oculus-iridis (Ehrenberg) Ehrenberg, 1840	+			0.06	43.81
Coscinodiscus radiatus Ehrenberg, 1840		+		0.51	50.62
Coscinodiscus sp.	+	+	+	0.66	58.48
Cyclotella sp.	+			16.50	7.99
Diatoma rhombica E.O'Meara, 1877	+			3.92	2.48
Diploneis elfvingiana var. latefurcata C.W.Fontell, 1917			+	0.25	4.80
Fragilaria nana Steemann Nielsen, 1935		+		44.17	1.63
Fragilariopsis curta (Van Heurck) Hustedt, 1958		+		**498.32**	40.10
Fragilariopsis cylindrus (Grunow) Krieger, 1954	+	+		**28990.13**	**570.19**
Fragilariopsis sp.	+	+	+	89.80	102.06
Grammatophora arcuata Ehrenberg, 1853	+			0.84	2.97
Haslea sp.	+	+		0.33	10.48
Licmophora abbreviata C.Agardh, 1831	+	+	+	3.35	43.04
Licmophora antarctica Carlson, 1913	+	+	+	7.07	281.35

Licmophora ehrenbergii (Kützing) Grunow, 1867	+	+		2.94	49.53
Licmophora sp.	+	+	+	18.74	17.01
Melosira antarctica Van Heurck, 1909		+		17.45	6.91
Melosira sp.		+	+	0.70	0.80
Navicula challengeri Grunow, 1880	+		+	0.16	5.74
Navicula cendronii Manguin, 1960	+	+		9.08	14.82
Navicula insuta Manguin, 1960	+	+		2.88	0.49
Navicula molesta Mann, 1925	+			0.38	0.16
Navicula sp.	+	+	+	180.20	174.74
Neomoelleria antarctica (Castrac.) S.Blanco & C.E.Wetzel, 2016	+			1.12	19.98
Nitzschia adeliana Manguin, 1960	+		+	1.35	1.41
Nitzschia capitellata Hustedt, 1922	+	+	+	1.15	0.50
Nitzschia longissima (Brébisson) Ralfs, 1861	+			1.27	0.21
Nitzschia sicula (Castracane) Hustedt	+			2.59	0.87
Nitzschia sp.	+	+	+	4.00	4.60
Nitzschia tenuirostris Mer.		+		0.07	0.01
Odontella aurita (Lyngbye) C.Agardh, 1832	+	+	+	3.32	**905.36**
*Odontella s*p.	+	+	+	7.41	408.16
Pinnularia directa var. directa W. Smith, 1853	+			14.34	39.13
Pinnularia sp.	+	+		0.13	12.86
Pleurosigma clevei Grunow, 1880	+	+	+	2.90	128.61
Pleurosigma sp.	+	+	+	1.61	65.31
Podosira vanheurckii var. vanheurckii M. Peragallo, 1921	+			0.42	9.21
Porosira glacialis (Grunow) Jörgensen, 1905		+	+	4.56	88.08
Proboscia alata (Brightwell) Sundström, 1986	+			1.96	29.20
Proboscia sp.	+			1.12	15.49
Pseudo-nitzschia delicatissima (Cleve) Heiden, 1928	+	+	+	43.48	19.41
Pseudo-nitzschia seriata (Cleve) H.Peragallo, 1899	+	+	+	79.86	27.64
Rhaphoneis fasciolata var. fasciolata Ehrenberg, 1844	+		+	0.12	5.72
Rhizosolenia imbricata Brightwell, 1858	+			0.79	7.49
Rhizosolenia truncata G.Karsten, 1905	+	+		8.91	180.89
Synedra adeliae Manguin, 1957	+	+	+	4.36	12.09
Synedra camtschatica var. antarctica Manguin, 1960	+	+	+	4.26	29.02
Synedra sp.	+	+	+	2.94	1.41
Thalassiosira australis M.Peragallo, 1921			+	0.09	2.88
Terebraria kerguelensis E.O'Meara, 1876 †	+	+	+	43.04	56.82
Thalassiosira antarctica Comber, 1896	+	+	+	72.98	286.03
Thalassiosira oliveriana (O'Meara) I.V.Makarova & V.A.Nikolajev, 1983	+	+		0.60	38.39
Thalassiosira rotula Meunier, 1910	+	+	+	30.61	23.32
Thalassiosira sp.	+	+	+	29.39	**581.94**
Thalassiothrix antarctica A.Schimper ex G.Karsten, 1905	+			0.27	7.25

Trachyneis aspera (Ehrenberg) Cleve, 1894			+	0.00	0.24
Trigonium arcticum (Brightwell) Cleve, 1868			+	0.00	3.62
Tropidoneis fusiformis E.Manguin, 1957	+			0.48	1.92
Chlorophyceae					
Ankistrodesmus antarcticus Kol & E.A.Flint, 1968		+	+	72.23	2.79
Chlorophyceae gen. sp.			+	1.61	5.68
Chlorophyceae gen. sp. 1		+	+	69.38	7.27
Chlorophyceae gen. sp. 2		+	+	30.87	11.80
Monoraphidium sp.	+	+		0.68	0.01
Coccolithophyceae					
Acanthoica acanthos J.Schiller, 1925	+	+		8.30	24.94
Emiliania huxleyi (Lohmann) W.W.Hay & H.P.Mohler, 1967	+			34.65	8.12
Phaeocystis antarctica Karsten, 1905	+			**4147.41**	**971.72**
Rhabdosphaera hispida Lohmann, 1912	+			0.68	1.49
Cryptophyceae					
Cryptomonas sp.	+			**1231.26**	128.68
Hillea fusiformis (J.Schiller) J.Schiller, 1925	+	+		**1554.89**	445.26
Cyanophyceae					
Cyanophyceae gen. sp.		+	+	0.68	0.53
Cyanophyceae gen. sp. 1		+		0.20	1.19
Johannesbaptistia pellucida (Dickie) W.R.Taylor & Drouet, 1938		+	+	0.06	0.68
Nostoc sp.		+		0.60	0.16
Oscillatoria tenuis C.Agardh ex Gomont, 1892		+		74.50	0.12
Dictyochophyceae					
Octactis speculum (Ehrenberg) F.H.Chang, J.M.Grieve & J.E.Sutherland, 2017	+	+	+	2.75	8.29
Dinoflagellata incertae sedis					
Protodinium simplex Lohmann, 1908	+			**411.95**	188.95
Dinophyceae					
Amphidinium crassum Lohmann, 1908	+		+	2.83	14.25
Glenodinium paululum Lindemann, 1928		+		1.27	3.36
Gymnodinium agiliforme Schiller, 1928	+			14.75	16.76
Gymnodinium biconicum J.Schiller, 1928	+			0.33	0.34
Gymnodinium najadeum J.Schiller, 1928	+			2.90	4.98
Gymnodinium sp.	+	+	+	28.44	55.77
Gymnodinium wulffii J.Schiller, 1933	+			35.36	18.41
Gyrodinium lacryma (Meunier) Kofoid & Swezy, 1921	+	+		20.66	143.97
Gyrodinium pingue (Schütt) Kofoid & Swezy, 1921	+			1.54	23.95
Gyrodinium sp.	+	+		0.65	0.54
Kapelodinium vestifici (Schütt) Boutrup, Moestrup & Daugbjerg, 2016	+	+		79.15	65.56
Oxytoxum turbo Kofoid, 1907		+		0.23	0.57
Pronoctiluca spinifera (Lohmann) Schiller, 1932	+			0.04	0.01

Prorocentrum micans Ehrenberg, 1834	+		0.44	0.46
Prorocentrum sp.	+	+	5.42	5.09
Protoperidinium smithii H.Doan-Nhu, L.Phan-Tan & L.Nguyen-Ngoc 2018	+	+	6.11	8.90
Scrippsiella acuminata (Ehrenberg) Kretschmann, Elbrächter, Zinssmeister, S.Soehner, Kirsch, Kusber & Gottschling, 2015	+		0.03	0.02
Euglenophyceae				
Euglena sp.		+	0.10	1.20
Mamiellophyceae				
Mantoniella sp.		+	0.30	0.00
Trebouxiophyceae				
Closteriopsis longissima (Lemmermann) Lemmermann, 1899	+	+	0.87	0.10
Ulvophyceae				
Hormidiopsis crenulata (Kützing) Heering, 1914	+	+	1.19	31.17

Table 1. Taxonomic list of phytoplankton in the waters of Argentine Islands, WAP (2019-2021).

Large-celled centric diatoms *Corethron criophilum* and *Corethron inerme* and the haptophyte *Phaeocystis antarctica* were dominant in terms of biomass (Table 1). Lower proportion of overall biomass was formed by representatives of *Odontella aurita*, *Thalassiosira sp.*, *Fragilariopsis cylindrus* and *Chaetoceros compressus* (Table 1). The largest total abundance was found for small-celled diatoms *Fragilariopsis cylindrus*, *Fragilariopsis curta* and *Chaetoceros compressus*, cryptophytes *Cryptomonas sp.*, *Hillea fusiformis* and *Phaeocystis antarctica*. Dinoflagellata *Protodinium simplex* reached significant abundances in 2019 (Table 1).

Representatives of the *Bacillariophyceae* have completely dominated in the phytoplankton of the Argentine Islands waters during the late summer periods of 2019, 2020 and 2021 (Fig. 3).

The lowest average contribution of diatoms to phytoplankton abundance (79%), biomass (79%) and surface area (93%) was observed in 2019. This is due to the significant development of *Coccolithophyceae*, accounting for up to 12% of the abundance and 10% of the biomass, and *Cryptophyceae*. The contribution of *Bacillariophyceae* to biomass and to the surface area increased to 97% and 98% respectively in the late summer period of 2020 and 2021 (Fig. 3). The representatives of *Coccolithophyceae* and *Cryptophyceae* were almost absent in the phytoplankton communities of 2020 and 2021. Instead, a moderate development of *Chlorophyceae* and undefined small-celled flagellate algae, with an average size of 12 μm and a volume of 470 μm^3, was observed and reached its maximum during the period of diatom decrease (Fig. 3).

The development of the most massive diatom – *Corethron criophilum* was a major factor behind the dynamics of phytoplankton biomass in the waters of the Argentine Islands during the late summer period of 2019, 2020 and 2021 (Fig. 4). This species was present during the entire period of research and significantly contributed to the increase in the community biomass, which reached its maximum at the end of March 2019, while also peaking in the second decade of February 2020,

March 2020, and March 2021 (Figs. 3, 4). The specific surface of *Corethron criophilum* was 218 $m^2 \cdot kg^{-1}$, which indicated the low potential functional capacity of this diatom (Zotov 2008). Additionally, the other large-celled diatoms with similar S/W values formed the majority of phytoplankton biomass in the late summer period. These are *Corethron inerme* (101 $m^2 \cdot kg^{-1}$), *Odontella aurita* (159 $m^2 \cdot kg^{-1}$), *Odontella sp.* (167 $m^2 \cdot kg^{-1}$), *Thalassiosira sp.* (232 $m^2 \cdot kg^{-1}$), *Porosira glacialis* (238 $m^2 \cdot kg^{-1}$) (Fig. 4). Thus, during the late summer seasons of all three years, the biomass was mainly formed by a group of large centric diatoms with a low S/W (from 70 to 300 $m^2 \cdot kg^{-1}$).

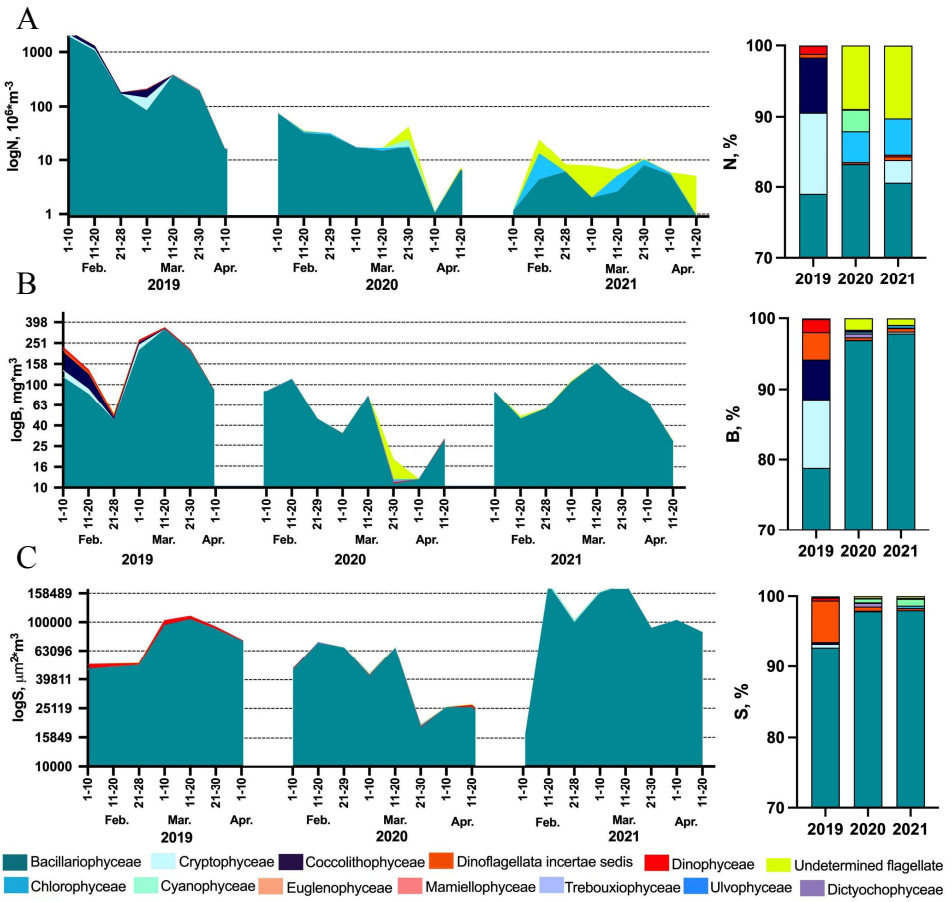

Fig. 3. Dynamics of the abundance (N), biomass (B) and surface area (S) of phytoplankton taxonomic groups in the waters of the Argentine Islands during the late summer period of 2019 – 2021 (*see* Supplementary, Table 3-5 for non-logarithmic values).

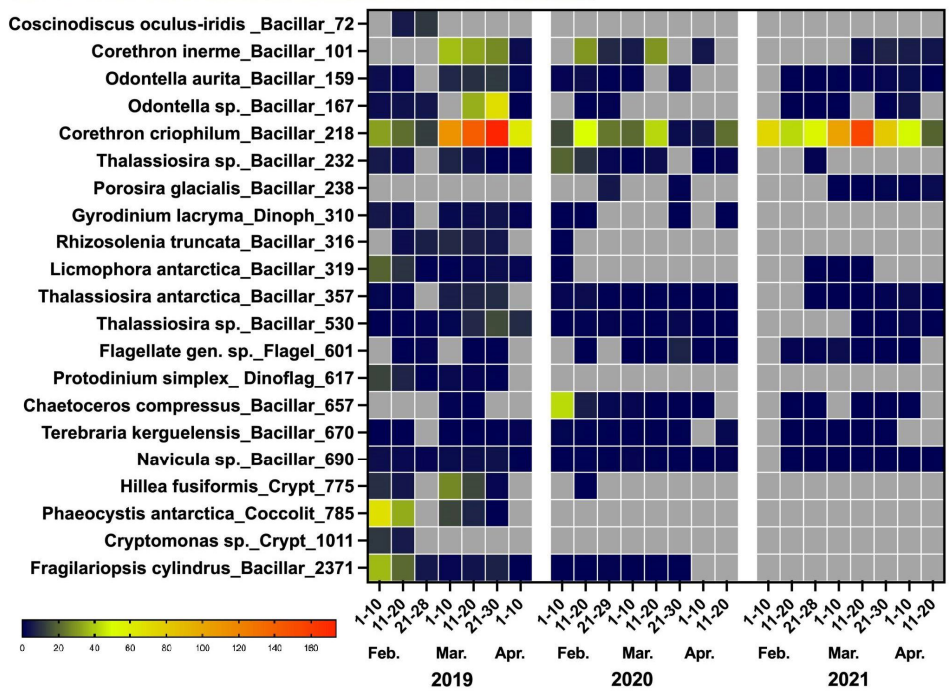

Fig. 4. Dynamics of the dominant phytoplankton species biomass ($mg \cdot m^{-3}$) in the waters of the Argentine Islands in late summer of 2019, 2020 and 2021 (X-axis: Decade – Month – Year; Y-axis: Species name - Taxonomic class - Specific surface value).

However, the nature of the late summer succession in 2019 and 2020 and 2021 was different. In 2019, the development of a group of small-celled species with specific surface values larger than 700 $m^2 \cdot kg^{-1}$ was observed. At the beginning of February 2019, high abundance of *Phaeocystis antarctica* (785 $m^2 \cdot kg^{-1}$), cryptophyte *Hillea fusiformis* (775 $m^2 \cdot kg^{-1}$) and *Cryptomonas sp.* (1011 $m^2 \cdot kg^{-1}$) and small-cell pennate diatom *Fragilariopsis cylindrus* (2371 $m^2 \cdot kg^{-1}$) (Fig. 4) was detected. The gradual decrease of this group abundance during February indicates that seasonal studies may have revealed the end of a more massive bloom. These species were found in very low quantity in the following years. The group of species with S/W from 300 to 700 $m^2 \cdot kg^{-1}$, including both diatoms and dinoflagellates, formed moderate biomass mainly during the late summer period of 2019 (Fig. 4). *Chaetoceros compressus* diatom (657 $m^2 \cdot kg^{-1}$) was the only one reaching a significant biomass in early February 2020. A moderate development of undetermined small-celled flagellate *Flagellate gen sp.* (601 $m^2 \cdot kg^{-1}$) was observed in March 2020, after the decline of *Corethron criophilum* abundance. Similar development of *Flagellate gen sp.* happened in March 2021, between the two peaks of *Corethron criophilum* biomass (Figs. 3, 4).

Phytoplankton taxonomic structure, revealed during the period of April 2020 – February 2021, was characterized by the overwhelming dominance of *Corethron criophilum*. The contribution of large centric diatoms, such as *Porosira glacialis*, *Odontella sp.* and *Thalassiosira sp.*, to the community biomass increased in the end of summer, while the ratio of dinoflagellata *Peridinium sp.* – at its beginning.

Metrics of phytoplankton development

The interannual dynamics of the average phytoplankton abundance (N), biomass (B), surface area (S) and surface index (ISC) was synchronous for the late summer seasons of 2019, 2020 and 2021 (Fig. 5). These metrics were found to be significantly higher in 2019, than in 2020 and 2021 (Supplementary, Table 2), except for S values, which did not differ in 2019 and 2021 (Supplementary, Table 2). 2020 was characterized by the lowest values for phytoplankton development metrics (except for the abundance). Thus, the late summer seasons of three consecutive years were characterized by a decrease of the phytoplankton quantitative development metrics in 2020, and their increase in 2021 to a level that did not exceed the values of 2019.

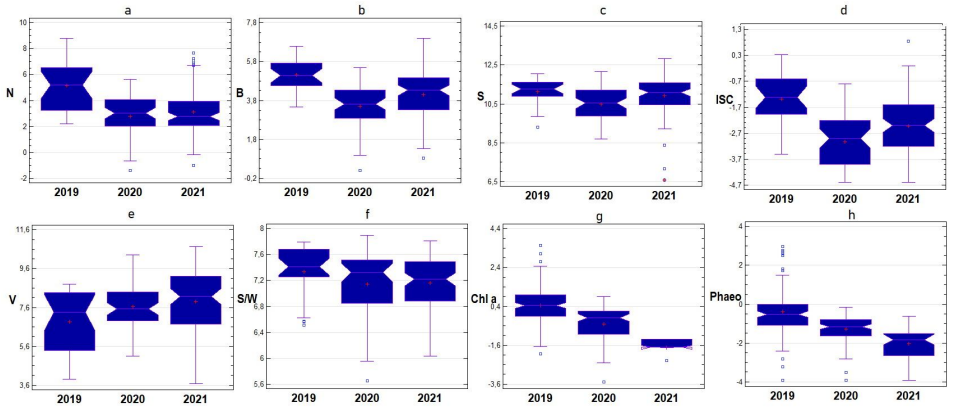

Fig. 5. Interannual variability of abundance (N, $10^6 \cdot m^{-3}$), biomass (B, $mg \cdot m^{-3}$), surface area (S, $mkm^2 \cdot m^{-3}$), surface index (ISC, m^{-1}), average cell volume (V, mkm^3), specific surface (S/W, $m^2 \cdot kg^{-1}$), concentrations of chlorophyll *a* (Chl a, $mg \cdot m^{-3}$) and phaeophytin (Phaeo, $mg \cdot m^{-3}$) of phytoplankton communities in the waters of the Argentine Islands in late summer period 2019-2021 (*see* Supplementary, Table 2 for Fisher's least significant difference).

The late summer dynamics of phytoplankton development metrics varied in different years (Fig. 6). A common feature was the presence of two peaks of phytoplankton development from the beginning of February to the end of April (Fig. 6). The biomass dynamics was most synchronous (Fig. 6b). After the minimum, observed from February 10 to March 10, in different decades depending on the year, an increase that reached a maximum on March 10-20 was detected, followed by a decrease to the April minimum (Fig. 6b). The ISC, which is most closely related to the gross primary production of phytoplankton (Zotov 2016), also reached maximum on March 10 – 20 in 2019 and 2020 (Fig. 6d). In 2021, the seasonal maximum values of the ISC were observed on February 21-30, while the March maximum of this metric was insignificant (Fig. 6d).

The dynamics of phytoplankton development, observed during the research from February 2020 to April 2021, indicates an early onset of the development. In 2020, the maximum of all metrics was observed in February (Fig. 7). In March 2020, a gradual decline began, reaching a minimum in June, changing little during the Antarctic winter.

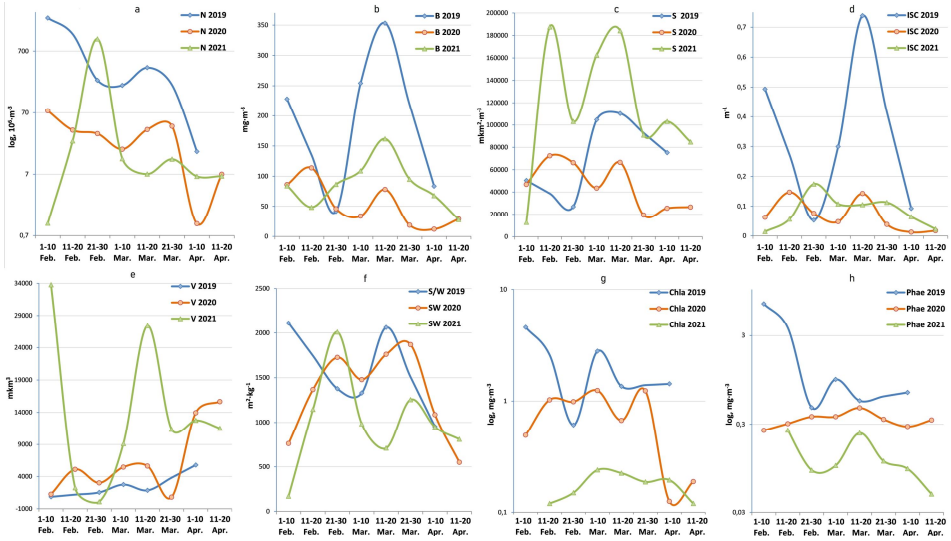

Fig. 6. Dynamics of abundance (N), biomass (B), surface area (S), surface index (ISC), average cell volume (V), specific surface area (S/W), chlorophyll *a* (Chla) and pheophytin (Phae) of phytoplankton communities in the waters of the Argentine Islands in the late summer period of 2019, 2020 and 2021 (*see* Supplementary, Table 6 for standard deviations).

In September 2020, a synchronous increase in began, reaching the first maximum in October (77 mg·m^{-3}), followed by a decline in December 2020 (to 43 mg·m^{-3}) (Fig. 7). From December to April 2021, two more successively increasing biomass maxima were observed: in January (98 mg·m^{-3}) and in March (125 mg·m^{-3}). Meanwhile, only one winter-spring maximum was observed in 2021 for the other development metrics: the abundance peaked in February, and the surface area and surface index peaked in March 2021 (Fig. 7).

Phytoplankton morphological structure

Morphological organization of phytoplankton in the Argentine Islands waters was characterized by a decrease in the communities' specific surface during the late summer periods of 2019, 2020 and 2021. S/W values in 2020 and 2021 were significantly lower than in 2019 (Fig. 5f; Supplementary, Table 2). This correlates with the opposite dynamics of a more traditional morphological metric – a cell volume, which was significantly bigger in 2019 than in 2020 and 2021 (Fig. 5e; Supplementary, Table 2). Phytoplankton S/W dynamics indicates a decrease in the potential intensity of production processes in 2020 and 2021. This could be potentially driven by a decrease in the presence of small, highly functional cryptophytes and *Phaeocystis antarctica* in late summer phytoplankton in 2020 and 2021 (Figs. 3, 4). Instead, the relative contribution of large-celled diatoms to the biomass of communities has increased by almost 20% for the late summer seasons of 2020 and 2021 (Fig. 3).

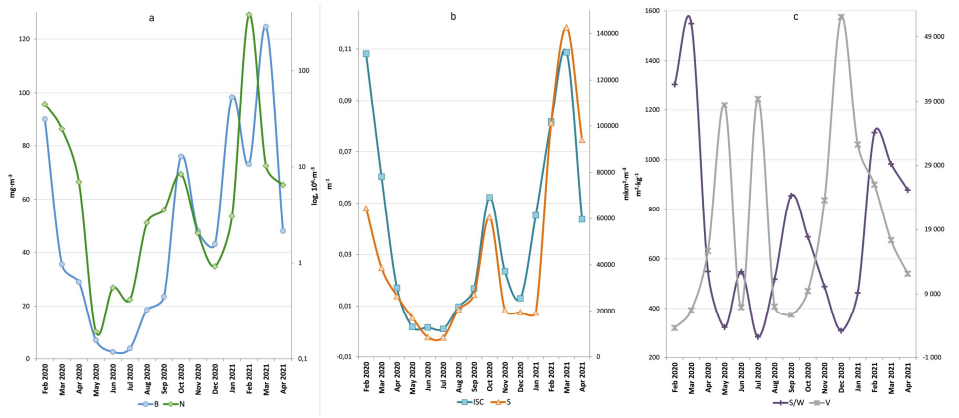

Fig. 7. Dynamics of average monthly abundance (N, $10^6 \cdot m^{-3}$), biomass (B, $mg \cdot m^{-3}$), surface area (S, $\mu m^2 \cdot m^{-3}$), surface index (ISC, m^{-1}), average cells' volume (V, mkm^3) and specific surface (S/W, $m^2 \cdot kg^{-1}$) of phytoplankton in the Argentine Islands waters in 2020-2021 (*see* Supplementary, Table 7 for standard deviations).

Morphological restructuring of phytoplankton is ensured both by the redistribution of different taxonomic groups' contributions to the communities' metrics, and by the variability of the size and shape of algae cells that form these groups. In the late summer seasons of 2020 and 2021, S/W for all mass taxonomic groups was lower than in 2019.

Indeed, the average specific surface of *Bacillariophyceae* cells was 2458 $m^2 \cdot kg^{-1}$, 1471 and 2068 $m^2 \cdot kg^{-1}$ in 2019, 2020 and 2021 respectively. The S/W of *Coccolithophyceae*, *Cryptophyceae* and *Dinoflagellata* decreased as well. Thus, the differences in phytoplankton morphological organization were associated with both a decrease in the presence of small-celled *Coccolithophyceae* and *Cryptophyceae* in the late summer seasons of 2020 and 2021 from 2019, as well as with a decrease in S/W of all mass groups of algae (such as *Bacillariophyceae*, *Coccolithophyceae, Cryptophyceae* and *Dinoflagellata*).

The intra-seasonal S/W dynamics were also different in three consecutive sampling years. Two phytoplankton specific surface maxima were observed (in the third decade of February and March) in 2020 and 2021 (Fig. 6f), whereas 2019 was characterized by the peak S/W values in early February and March 2019 (Fig. 6f). A decrease in communities' S/W was observed from 1549 to 323 $m^2 \cdot kg^{-1}$ during March-May 2020 (Fig. 7), followed by two similar minima, which were replaced by gradually increasing peaks of S/W from spring to summer – in June 2020 (548 $m^2 \cdot kg^{-1}$), in September 2020 (855 $m^2 \cdot kg^{-1}$) and in February 2021 (1112 $m^2 \cdot kg^{-1}$) (Fig. 7c). This confirms the morphological restructuring of Antarctic phytoplankton groups associated with the successive increase in the intensity of production processes from winter to summer, alternating with the periods of low-activity algae dominance.

Chlorophyll concentrations

Gradual and significant decrease of the average chlorophyll *a* (from 2.81 to 0.16 $mg \cdot m^{-3}$) and pheophytin (from 2.82 to 0.19 $mg \cdot m^{-3}$) concentration was observed in the late summer periods of 2019, 2020 and 2021 (Fig. 5, g, h; Supplementary, Ta-

ble 2). Both chlorophyll *a* and pheophytin values correlated positively with phytoplankton biomass – R = 0.65, $p<0.05$ and R = 0.34, $p<0.05$ respectively. Yet, the relationship between the biomass and chlorophyll *a* concentration was different during 3 consecutive years (Fig. 8a). This may be driven by inter-seasonal differences in phytoplankton morphological organization, which, alongside with the communities' functional traits, determine the specific contribution of chlorophyll per unit of biomass. The intra-seasonal variability of pigment concentrations for late summer periods of different years had an individual character and was not characterized by common features (Fig. 6g, h).

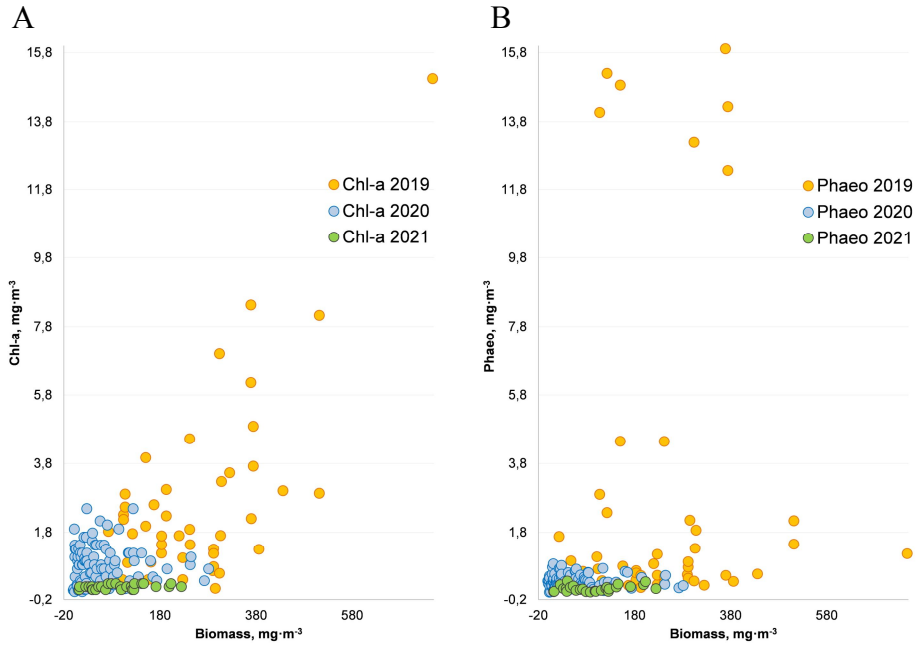

Fig. 8. Distribution of chlorophyll *a* and pheophytin concentration depending on the phytoplankton biomass in the Argentine Islands waters in the late summer period of 2019, 2020 and 2021.

Discussion

Species diversity of phytoplankton in the waters of the Argentine Islands

The relatively low phytoplankton species diversity detected in the Argentine Islands waters during the late summer of 2019 – 2021 is in line with the previous results. The list of unicellular algae species of this area was gradually supplemented starting with the first seasonal surveys in March 1997, which revealed 23 species of diatoms (Ivanov and Minicheva 1998). 70 phytoplankton taxa were identified in this water area in the fall of 1998 (Seryogin et al. 2003), 136 taxa – in the fall of 2002 (Kuzmenko 2004), and 64 taxa – in the fall of 2004 (Gerasimyuk 2008). Longer annual research (2002 – 2003) revealed 126 species of phytoplankton (Kuzmenko

and Ignatiev 2007, 2008). This list was supplemented in 2005 with the other 31 taxa (Kuzmenko and Ignatiev 2007, 2008). 105 and 115 species were identified in the water area of Galindez island in 2005 − 2006 and 2006 − 2007, respectively (Kuzmenko and Ignatiev 2012). The general list of phytoplankton and benthic species found in the surface water layer of the Argentine Islands archipelago contained 199 taxa (Kuzmenko and Ignatiev 2012). These estimates are close to the phytoplankton species diversity at the shelf zone of the Antarctic Peninsula, the South Shetland Islands, the Bransfield and Drake Straits, and the ice-free waters of the Bellingshausen Sea (Kuzmenko and Ignatiev 2012, Bidigare et al. 2001). The diversity of phytoplankton reached 66 species in the water area of the Argentine Islands during the late summer of 2005, and the average for different seasons was 63 taxa (Kuzmenko and Ignatiev 2006, 2008). This corresponds to the average species richness detected in the late summer period of 2019 – 2021 (77 taxa). Thus, the 2019 – 2021 research did not reveal significant changes in the species diversity of the research area.

Succession of phytoplankton in the waters of the Argentine islands

Phytoplankton development cycles are determined by annual cycles of solar activity in the southern latitudes (Clarke et al. 2008, Ducklow et al. 2012). Late summer decline in the WAP phytoplankton development is followed by a winter decline in biomass with a predominance of picoplankton (Clarke et al. 2008, Rozema et al. 2017). An increase in daylight, in the angle of solar inclination and in the ice-free area accompanying spring leads to elevated light availability and activates algal growth. Ice melting contributes to the formation of a stable ocean surface layer of lower density, high temperature and high biogenic elements content. This summer stratification creates favourable conditions for the rapid algal development (Clarke et al. 2008, Venables et al. 2013, Vernet et al. 2008) and is considered to be a major driver of phytoplankton productivity (Garibotti et al. 2005a, Vernet et al. 2008). Indeed, macronutrients and micronutrients in the WAP coastal waters are generally considered abundant, due to the input from glaciers and upper circumpolar deep water layers (Annett et al. 2017, Sherrell et al. 2018, Carvalho et al. 2020).

Diatoms, cryptophytes, haptophytes, prasinophytes and mixed flagellates constitute the majority of coastal phytoplankton in the WAP waters (Varela et al. 2002, Garibotti et al. 2005a, Schofield et al. 2017). Diatoms are a dominant taxonomic group (Mitchell and Holm-Hansen 1991, Prézelin et al. 2000, Schofield et al. 2017, Rozema et al. 2017). In addition, periodic blooms are caused by *Phaeocystis antarctica* (Annett et al. 2010) and cryptophytes, with more and more frequent mass development (Montes-Hugo et al. 2009, Schofield et al. 2017).

The first systematic seasonal phytoplankton monitoring in the waters of the Argentine Islands was conducted from April 2002 to February 2003 (Seregin et al. 2005, Kuzmenko and Ignatiev 2007). A gradual decrease in algal abundance (from 146.9 to 0.1 $10^6 \cdot m^{-3}$) and biomass (from 168.0 to 0.1 $mg \cdot m^{-3}$) was detected from the beginning of April to July 2002 (Fig. 9) (Kuzmenko and Ignatiev 2007). An intense *Phaeocystis pouchetii (Hariot) Lagerh* bloom (up to 108 $10^9 \cdot m^{-3}$ and 12.3 $g \cdot m^{-3}$) staring the beginning of the Antarctic spring (September 2002), peaking in mid-October and collapsing in November 2002 was observed. The biomass was formed by large diatoms from the *Coscinodiscus*, *Odontella*, *Membraneis*,

Thalassiora, and *Charcotia* genera during this period. In November – December, *Fragilariopsis*, *Achnanthes*, and *Corethron* dominated (2.2 $10^9 \cdot m^{-3}$; 3.2 $g \cdot m^{-3}$) (Kuzmenko and Ignatiev 2007). Phytoplankton structure changed significantly, accompanied by a decrease of its biomass (43.7 – 11.9 $10^6 \cdot m^{-3}$ and 93.0 – 12.1 $mg \cdot m^{-3}$) at the beginning of January 2003. Subsequently, the development of large (330 – 650 μm^3) flagellates from the *Cryptomonas* (*Cryptophyta*) and *Pyramimonas* (*Chlorophyta*) genera (1 $10^9 \cdot m^{-3}$ and 350 $mg \cdot m^{-3}$ respectively) began in mid-January. The development of these algae was much more massive (up to 300 $10^9 \cdot m^{-3}$ and 120 $g \cdot m^{-3}$) in the adjacent waters of Petermann Island. A prominent decrease of phytoplankton abundance and diversity was observed by the end of January (Fig. 9; Kuzmenko and Ignatiev 2007). Thus, three phytoplankton development phases, differing in abundance, biomass, diversity and size structure have been detected during the spring-summer season of 2002 – 2003: the October bloom, caused by *Phaeocystis*, was followed by the development of large diatoms in November, and by representatives of *Cryptomonas*, *Pyramimonas* and small flagellates in mid-January (Kuzmenko and Ignatiev 2007, 2008).

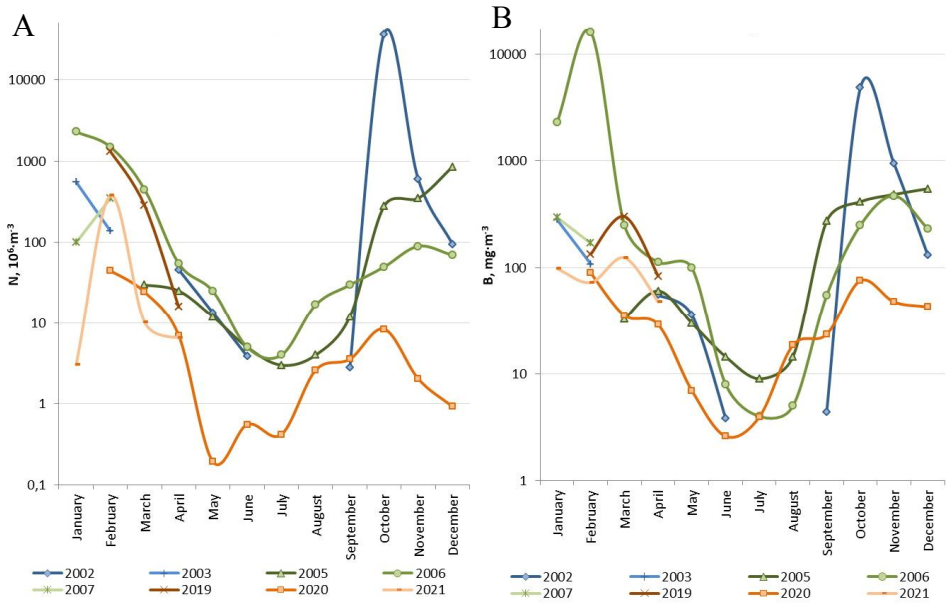

Fig. 9. Monthly phytoplankton abundance (N, $10^6 \cdot m^{-3}$) and biomass (B, $mg \cdot m^{-3}$) in the Argentine Islands waters in 2002-2003 and 2005-2007 (according to Kuzmenko and Ignatiev 2007, 2008, 2012) and 2020-2021.

A slightly different nature of phytoplankton development was witnessed in the waters of the Argentine Islands in 2005 – 2007 (Fig. 9) (Kuzmenko and Ignatiev 2012). The phytoplankton abundance and biomass gradually decreased to 1.4 $10^6 \cdot m^{-3}$ and 3.7 $mg \cdot m^{-3}$ from March to August 2005 with subsequent increase up to 214 $10^6 \cdot m^{-3}$ and 487 $mg \cdot m^{-3}$ in September – November 2005 (mainly due to the development of *Fragillariopsis* species). A bloom event was observed in summer during December 2005 – January 2006 accompanied by a peak biomass

of 2.9 $10^9 \cdot m^{-3}$ (Fig. 9). Small flagellates, as well as *Dunaliella*, *Pyramimonas* and *Cryptomonas* representatives constituted up to 61% of the abundance during this period. Meanwhile, medium and large species of diatoms (*Odontella*, *Proboscia*, *Eucampia*, *Thalassiosira* genera) accounted for up to 90% of the total biomass, and increased considerably in their biomass in response to higher water temperature, forming the most intense diatom bloom in the whole study period (up to 29.4 $g \cdot m^{-3}$; Fig. 9). The community biomass decreased to 349 $mg \cdot m^{-3}$, and the abundance (up to 85% of which was formed by *Fragilariopsis*) – to 434 $10^6 \cdot m^{-3}$ at the beginning of March 2006. Phytoplankton biomass was still mainly formed by large diatoms *Corethron*, *Trachyneis*, *Haslea*, *Membraneis* and *Proboscia* in April – May, but dropped to 14 $mg \cdot m^{-3}$, while the abundance – to 4 $10^6 \cdot m^{-3}$. No mass phytoplankton development was observed in the spring-summer season of 2006 – 2007, and the average biomass was 25 times lower than the year before, with a similar species composition (Kuzmenko and Ignatiev 2012 .

Thus, in contrast to the mass development in October 2002, low occurrence of *Phaeocystis* was detected in the spring of 2005, and it was almost absent in November 2006. *Fragillariopsis* abundance increased significantly in 2005 compared to 2002 – 2003, while becoming an order of magnitude lower in the spring of 2006. The diatom *Achnanthes brevipes*, dominant in October – November 2002, was almost never found in the spring of 2005 and 2006. *Corethron criophilum*, which constituted up to 70% of biomass in autumn-winter of 2002, was also found in small quantities during 2005 – 2006 (Kuzmenko and Ignatiev 2012).

The dynamics of phytoplankton development revealed in the current study in 2019 – 2021 was comparable to previous results gained in the waters of the Argentine Islands. The quantitative development metrics of late summer phytoplankton were found to be rather close in different periods. Thus, the average biomasses in February 2019 – 2021 are comparable to similar metrics in February 2003 and 2007, while the March biomasses of 2019 – 2021 correspond to the values observed in March 2005 and 2006. Naturally, the April biomasses of 2019 – 2021 are very close to similar values in April 2002, 2005 and 2006 (Fig. 9). The taxonomic structure of phytoplankton communities was found to be very similar during the corresponding periods of different years. Indeed, the main dominant group was large centric diatoms, with a significant contribution of smaller pennate diatoms (*Fragilariopsis*) and flagellate algae. Thus, the development of phytoplankton from February to April 2019 – 2021 corresponded to the results of previous studies, both quantitatively and qualitatively.

Nevertheless, the phytoplankton development found from February 2020 to February 2021 were lower than those in 2002 – 2007. This period was characterized by the minimum values of average monthly biomass for the entire period of phytoplankton research in the waters of the Argentine Islands. The exception was the winter-spring, as the biomass in August and September 2020 exceeded similar values of 2002, 2005, and 2006. But no bloom or even a significant phytoplankton development dominated by large centric diatoms was detected in the samples taken during the Antarctic spring of 2020. Instead, smaller *Fragilariopsis cylindrus* and *Chaetoceros sp.* with a rather low occurrence of undetermined flagellate were forming the maximum abundance during this period. Our two-week sampling periodicity leaves high probability of missing significant events in the phytoplankton development, so this atypical nature of the annual succession requires a more detailed analysis.

Hence, fairly clear patterns of phytoplankton annual succession can be detect-

ed in Argentine islands waters. After the winter decline, when the average biomass decreases to the 1-10 $mg \cdot m^{-3}$, spring development begins, usually with high abundances of *Fragilariopsis* representatives and with a predominant contribution of the large centric diatoms to the biomass. At the beginning of summer, the role of *Cryptomonas* (*Cryptophyta*), *Pyramimonas* (*Chlorophyta*) and small flagellates increases. The average spring-summer biomass varies from 100 to 1000 $mg \cdot m^{-3}$. The dominance of large centric diatoms is established again in the late summer period, accompanied by a significant presence of small flagellates and a periodic increase in *Fragilariopsis* contribution. The average biomass gradually decreases during the Antarctic autumn, being in the range from 10 to 100 $mg \cdot m^{-3}$ in April – May. A decrease in the phytoplankton development and in the role of flagellates was observed in 2020 – 2021, but the relatively low sampling frequency reduces the possibilities to interpret this data.

Only two notable exceptions have been recorded during the entire period of phytoplankton research in the Argentine Islands waters, with the single-celled algae biomass exceeding 1 $g \cdot m^{-3}$. This was the spring bloom of *Phaeocystis* in October 2002 and the biomass "flash" in February 2006, formed by large centric diatoms with a significant abundance of flagellate algae.

Phytoplankton succession of the WAP area adjacent to the Argentine islands

Despite common features, the development of phytoplankton in different areas of the WAP shows significant interannual and regional variability, which can be driven by the complex effect of the regional ice conditions of the preceding winter and by the wind activity. It is hypothesized that the years with less sea ice and stronger wind mixing lead to larger input of nutrients from deeper layers to surface waters (Annett et al. 2010). On the other hand, less deep water column mixing driven by moderate wind activity and high sea ice extent requires less solar energy to stabilize it in the following summer (Venables et al. 2013). Furthermore, more algal biomass can accumulate in more stratified waters, leading to phytoplankton blooms (van Leeuwe et al. 2020). Recent climate change consequences are also affecting phytoplankton succession in the WAP waters (van Leeuwe et al. 2020). Comparison of the phytoplankton dynamics in the Argentine Islands waters in 2019 – 2021 with the processes detected in the adjacent areas of the WAP in previous years can contribute to understanding of the regional trends.

Research conducted south of the Argentine Islands, at Rothera Station in Ryder Bay in 2012 – 2017 revealed clear patterns of phytoplankton succession (van Leeuwe et al. 2020). Two consecutive blooms were observed for four out of the total five observation years, following previously described patterns (Clarke et al. 2008, Annett et al. 2010). Multi-year data confirmed a clear species succession between November and March. Autotrophic flagellates (haptophytes, chlorophytes, and prasinophytes), most likely derived from sea ice communities, were dominant in spring and gradually declined by January. *Chrysochromulina sp.*, *Micromonas sp.*, *Pyramimonas spp*. and *Phaeocystis antarctica* were dominating. Diatoms peaked in more stratified and warmer surface waters from January to March. In January – February, small centric diatoms *Thalassiosira sp.* (< 20 μm) were quite common, but such large centric species as *Proboscia inermis* and *Corethron sp.* formed the major biomass. In January, a significant abundance of small cryptophytes (5 – 20 μm) with strong signs

of mixotrophy were also observed, whereas dinoflagellates were present in very low abundance (van Leeuwe et al. 2020). However, significant interannual fluctuations associated with differences in wind mixing, ice cover, and El Niño were detected, which began in December 2015 and had a strong impact on processes in the WAP (van Leeuwe et al. 2020). High chlorophyll content was observed in 2013 and 2017 under conditions of a shallow summer mixed layer (van Leeuwe et al. 2020). The intervening 2014 – 2016 years were characterized by low biomass, which contradicts the hypothesis of the link between heavy winter sea ice cover and subsequent high summer phytoplankton biomass (Venables et al. 2013).

Remarkably similar annual phytoplankton successional patterns driven by constant seasonal factors (*e.g.*, solar radiation, temperature, and freshwater input) were shown at the Palmer Station, located north of the Argentine Islands (2017 – 2019), while storm/wind events caused more ephemeral interannual differences (Nardelli et al. 2023). A shorter sea ice season with early rapid ice retreat was associated with low phytoplankton biomass and reduced diatom contributions (2017 – 2018), whereas a longer sea ice season with late ice retreat resulted in the opposite (2018 – 2019) (Nardelli et al. 2023). Consistent seasonal succession patterns were detected despite significant interannual differences in sea ice dynamics and phytoplankton biomass (Nardelli et al. 2023). They correspond to earlier studies in the coastal WAP (Schofield et al. 2017, Garibotti et al. 2005a), but differ from those found in the Rothera station area (van Leeuwe et al. 2020).

Three main successive phases of phytoplankton development were defined for the Palmer Station area: spring ice retreat phase, peak summer phase and late summer phase. The spring ice retreat phase (November-December) was characterized by blooms dominated by large centric diatoms associated with the spring sea ice retreat and upper water layer stratification. This phase was marked by a high abundance of centric diatoms (55% of the total biovolume), prasinophytes *Pyramimonas spp.* (5% of biovolume) and *P. antarctica* haptophytes (3% of biovolume) in 2017 – 2019 (Nardelli et al. 2023). Large spring blooms of centric diatoms have been observed in other Antarctic studies (Garibotti et al. 2005 a,b; Costa et al. 2020, 2021). Yet, these events are significantly different from the succession at the Rothera station, where the initial phase starts with the flagellates – *Pyramimonas spp*. and *Phaeocystis antarctica*, and is fuelled by the sea ice melt (van Leeuwe et al. 2020, 2022). These species were also observed in relatively high abundance at the Palmer station during the spring ice retreat phase, but there relative dominance was not pronounced. There was a rapid increase in centric diatoms such as *Thalassiosira spp.* and *Chaetoceros spp.*, which are absent in sea ice and gain advantage from the optimal light conditions provided by stratification (Nardelli et al. 2023).

The peak summer phase (December-January), accompanied by reduced nutrient reserves, is characterized by the prevalence of mixotrophic cryptophytes with low chlorophyll *a* content. The lowest chlorophyll *a* concentrations, yet the highest biovolume and abundance values, were recorded during the peak summer phase of 2017 – 2019. It was associated with abundant cryptophytes (29% biovolume), mixed flagellates (27% biovolume) and unidentified small-celled pennate diatoms, probably *Fragilariopsis spp.* and *Nitzschia spp.* (19% biovolume) (Nardelli et al. 2023). The vigorous development of these pennate diatoms produced almost twice as much biomass as any other bloom during the study period (Nardelli et al. 2023).

During the late summer phase (February-March), small (< 20 μm) diatoms and mixed flagellates, including haptophytes and undetermined flagellates, dominated

(Nardelli et al. 2023). The late summer phase was associated with a relatively high abundance of centric diatoms (47% of biovolume) and mixed flagellates (30% of biovolume). 46% of the centric diatoms were unidentified disc-shaped cells 15 to 20 μm in diameter (probably of the genus *Thalassiosira*). Species of pennate diatoms, including *Cocconeis spp.* and *Licmophora spp.*, had the highest abundance during this phase (Nardelli et al. 2023).

In summary, common features of phytoplankton development can be detected along the WAP. The October 2002 *Phaeocystis* bloom in Argentine Islands waters corresponds to the first stage detected at the Rothera station, while in all subsequent years the spring-summer development of phytoplankton was close to that described in the studies at the Palmer station. However, the late summer phase at the Palmer station area is almost not manifested in the waters of the Argentine Islands, except for 2019, when *Phaeocystis antarctica*, cryptophyte *Hillea fusiformis* and *Cryptomonas sp.* developed at the end of summer. The development of phytoplankton during this period corresponded to the stage of succession, more typical for southern Ryder Bay. Further monitoring has a potential to reveal changes occurring in the organization of marine phytoplankton communities under the impact of climate change.

Conclusion

121 species and intraspecific taxa of unicellular algae belonging to 12 taxonomic classes were found in the waters of the Argentine Islands during the late summer of 2019 – 2021. *Bacillariophyceae* completely dominated the studied phytoplankton community. The biomass dynamics was largely determined by the development of the most massive diatom *Corethron criophilum* and a complex of other large-celled centric diatoms with low specific surface values (70 – 300 $m^2 \cdot kg^{-1}$). The nature of late summer succession was typical for the Argentine Islands waters in 2019, 2020 and 2021. However, in contrast to 2020 and 2021, a more significant development of small-celled species with specific surface values exceeding 700 $m^2 \cdot kg^{-1}$ (haptophyte *Phaeocystis antarctica* (785 $m^2 \cdot kg^{-1}$), cryptophytic *Hillea fusiformis* (775 $m^2 \cdot kg^{-1}$) and *Cryptomonas sp.* (1011 $m^2 \cdot kg^{-1}$), as well as small-celled pennate diatom *Fragilariopsis cylindrus* (2371 $m^2 \cdot kg^{-1}$)) was observed in 2019. The lowest metrics of phytoplankton development along with the simplified community structure were detected during April 2020 – February 2021. Specific surface values were significantly lower in late summer 2020 and 2021 than in 2019 indicating a lower intensity of functional processes.

Clear annual succession patterns have been detected in Argentine Islands' phytoplankton communities. The winter recession with the average biomass drop to 1-10 $mg \cdot m^{-3}$ was followed by spring development, associated with high *Fragilariopsis* abundance and predominant contribution of large centric diatoms. The role of a *Cryptomonas* (Cryptophyta), *Pyramimonas* (Chlorophyta) and small flagellates increased at the beginning of summer. Subsequently, the dominance of large centric diatoms with a significant presence of small flagellates and a periodic increase in the contribution of *Fragilariopsis* was established in late summer period.

Phytoplankton development observed in Argentine Islands' waters resembled the processes detected in different geographically close regions along the WAP, namely the Rothera and Palmer stations, yet was characterized by certain peculiarities. Further observations might shed the light on the impact of climate change on marine phytoplankton communities.

References

ANNETT, A. L., CARSON, D. S., CROSTA, X., CLARKE, A. and GANESHRAM, R. S. (2010): Seasonal progression of diatom assemblages in surface waters of Ryder Bay, Antarctica. *Polar* Biology, 33: 13-29. doi: 10.1007/s00300-009-0681-7

ANNETT, A. L., HENLEY, S. F., VENABLES, H. J., MEREDITH, M. P., CLARKE, A. and GANESHRAM, R. S. (2017): Silica cycling and isotopic composition in northern Marguerite Bay on the rapidly-warming western Antarctic Peninsula. *Deep Sea Research Part II: Topical Studies in Oceanography*, 139: 132-142. doi: 10.1016/j.dsr2.2016.09.006

ARRIGO, K. R., VAN DIJKEN, G. L. and BUSHINSKY, S. (2008): Primary production in the Southern Ocean, 1997-2006. *Journal of Geophysical Research: Oceans*, 113: C08004. doi: 10.1029/2007JC004551

ARRIGO, K. R., VAN DIJKEN, G. L., ALDERKAMP, A. C., ERIKSON, Z. K., LEWIS, K. M., LOWRY, K. E., JOY-WARREN, H. L., MIDDAG, R. and *others* (2017): Early spring phytoplankton dynamics in the western Antarctic Peninsula. *Journal of Geophysical Research: Oceans*, 122: 9350-9368. doi: 10.1002/2017JC013281

BIDIGARE, R. R., IRIARTE, J. L., KANG, S. H. and *others* (2001): Phytoplankton: quantitative and qualitative assessments. Found. Ecolog. Res. west of the Antarctic peninsula. *Antarctic Research Series*, 70: 173-198.

CARVALHO, F., FITZSIMMONS, J. N., COUTO, N., WAITE, N., GORBUNOV, M., KOHUT, J., OLIVER, M. J., SHERRELL, R. M. and SCHOFIELD, O. (2020): Testing the canyon hypothesis: Evaluating light and nutrient controls of phytoplankton growth in penguin foraging hotspots along the West Antarctic Peninsula. *Limnology and Oceanography*, 65: 455-470. doi: 10. 1002/lno.11313

CLARKE, A. M., MEREDITH, P., WALLACE, M. I., BRANDON, M. A. and THOMAS, D. N. (2008): Seasonal and interannual variability in temperature, chlorophyll and macronutrients in northern Marguerite Bay, Antarctica. *Deep Sea Research Part II: Topical Studies in Oceanography*, 55: 1988-2006. doi: 10.1016/j.dsr2.2008.04.035

COOK, A. J., HOLLAND, P. R., MEREDITH, M. P., MURRAY, T., LUCKMAN, A. and VAUGHAN, D. G. (2016): Ocean forcing of glacier retreat in the western Antarctic Peninsula. *Science*, 353: 283-286. doi: 10.1126/science.aae0017

COSTA, R. R., MENDES, C. R. B., FERREIRA, A., TAVANO, V. M., DOTTO, T. S. and SECCHI, E. R. (2021): Large diatom bloom off the Antarctic peninsula during cool conditions associated with the 2015/2016 El Niño. *Communications Earth & Environment*, 2: 252. doi: 10.1038/s43247-021-00322-4

COSTA, R. R., MENDES, C. R. B., TAVANO, V. M., DOTTO, T. S., KERR, R., MONTEIRO, T., ODEBRECHT, C. and SECCHI, E. R. (2020): Dynamics of an intense diatom bloom in the Northern Antarctic Peninsula, February 2016. *Limnology and Oceanography*, 65: 2056-2075. doi: 10.1002/lno.11437

DEPPELER, S. L., DAVIDSON, A. T. (2017): Southern Ocean phytoplankton in a changing climate. *Frontiers in Marine Science*, 4: 40. doi: 10.3389/fmars.2017.00040

DUCKLOW, H. W., FRASER, W. R., MEREDITH, M. P., STAMMERJOHN, S. E., DONEY, S. C., MARTINSON, D. G., SAILLEY, S. F., SCHOFIELD, O. M., STEINBERG, D.K., VENABLES, H. J. and AMSLER, C. D. (2013): West Antarctic Peninsula: An ice-dependent coastal marine ecosystem in transition. *Oceanography*, 26: 190-203. doi: 10.5670/oceanog.2013.62

DUCKLOW, H. W., CLARKE, A., DICKHUT, R., DONEY, S. C., GEISZ, H., HUANG, K., MARTINSON, D. G., MEREDITH, M. P. and *others* (2012): The marine system of the Western Antarctic Peninsula. *In*: A. D. Rogers, N. M. Johnston, E. J. Murphy, and A. Clarke (eds.): Antarctic Ecosystems. Chichester, United Kingdom: John Wiley and Sons, Ltd.. 121–159.

GARIBOTTI, I. A., VERNET, M. and FERRARIO, M. E. (2005a): Annually recurrent phytoplanktonic assemblages during summer in the seasonal ice zone west of the Antarctic Peninsula (Southern Ocean). *Deep Sea Research Part I: Oceanographic Research Papers*, 52: 1823-1841. doi: 10.1016/j.dsr.2005.05.003

GARIBOTTI, I. A., VERNET, M., SMITH, R. C. and FERRARIO, M. E. (2005b): Interannual variability in the distribution of the phytoplankton standing stock across the seasonal sea-ice zone west of

the Antarctic Peninsula. *Journal of Plankton Research*, 27: 825-843. doi: 10.1093/plankt/fbi056

GERASYMIUK, V. P. (2008): Algae of marine littoral and inland water bodies of Galindez Island (Argentine Islands, Antarctic). *International Journal on Algae*, 10(1): 1-13. doi: 10.1615/InterJAlgae.v10.i1.10

HENLEY, S. F., SCHOFIELD, O. M., HENDRY, K. R., SCHLOSS, I. R., STEINBERG, D. K., MOFFAT, C., PECK, L. S., COSTA, D. P. and *others* (2019): Variability and change in the west Antarctic Peninsula marine system: Research priorities and opportunities. *Progress in Oceanography*, 173: 208-237. doi: 10.1016/j.pocean.2019.03.003

HENSON, S. A., BANLIEU, C. and LAMPITT, R. (2016): Observing climate change trends in ocean biogeochemistry: When and where. *Global Change Biology*, 22: 1561-1571.

HUGHES, C., CHUCK, A. L., ROSSETTI, H., MANN, P. J., TURNER, S. M., CLARKE, A., CHANCE, R. and LISS, P. S. (2009): Seasonal cycle of seawater bromoform and dibromomethane concentrations in a coastal bay on the western Antarctic Peninsula. *Global Biogeochemical Cycles*, 23: GB2024. doi: 10.1029/2008GB003268

IVANOV, A. I., MINICHEVA, G. G. (1998): Planktonic and benthic algae of the area of the Ukrainian Antarctic station «Akademik Vernadsky». *Bulletin of the Ukrainian Antarctic Center*, 2: 198-203.

KAŇA, R., KOTABOVÁ, E., SOBOTKA, R. and PRÁŠIL, O. (2012): Nonphotochemical quenching in cryptophyte alga Rhodomonas salina is located in chlorophyll a/c antennae. *PLoS One*, 7: e29700. doi: 10.1371/journal.pone.0029700

KHRYSTIUK, B., GORBACHOVA, L., SHPYG, V. and PISHNIAK, D. (2022): Changes in extreme temperature indices at the Ukrainian Antarctic Akademik Vernadsky station, 1951-2020. *Meteorology Hydrology and Water Management*, 10(1): 95-106. doi: 10.26491/mhwm/150883

KIM, H., DUCKLOW, H. W., ABELE, D., RUIZ BARLETT, E. M., BUMA, A. G. J., MEREDITH, M. P., ROZEMA, P. D., SCHOFIELD, O. M., VENABLES, H. J. and SCHLOSS, I. R. (2018): Inter-decadal variability of phytoplankton biomass along the coastal West Antarctic Peninsula. *Philosophical transactions. Series A, Mathematical, Physical, and Engineering Sciences*, 376: 20170174. doi: 10.1098/ rsta.2017.0174

KUZMENKO, L. V. (2004): Phytoplankton of the western Bransfield Strait. *Ukrainian Antarctic Journal*, 2: 125-137. doi: 10.33275/1727-7485.2.2004.607

KUZMENKO, L. V., IGNATIEV, S. M. (2006): Seasonal variability of species composition and quantitative development of phytoplankton in the area of the Antarctic station «Akademik Vernadsky». Scientific research in the Antarctic: III Intern. conf. Kyiv. 133.

KUZMENKO, L. V., IGNATIEV, S. M. (2007): Seasonal variability of the quantitative development of phytoplankton in the Argentine Islands (Antarctica). *Marine Ecology Journal,* 6(3): 47-60.

KUZMENKO, L. V., IGNATIEV, S. M. (2008): Species diversity of phytoplankton in the waters of the Argentine Islands (Antarctica). *Algology*, 18(2): 198-212.

KUZMENKO, L. V., IGNATIEV, S. M. (2012): Phytoplankton in the waters of Galindez Island (Argentine Islands, Antarctica) *Morskiy Ekologichnyi Zhurnal*, 2(XI): 53-63.

LEGGE, O. J., BAKKER, D. C. E., MEREDITH, M. P., VENABLES, H. J. and BROWN, P. J. (2017): The seasonal cycle of carbonate system processes in Ryder Bay, West Antarctic Peninsula. *Deep-Sea Research Part II: Topical Studies in Oceanography*, 39: 167-180. doi: 10.1016/j.dsr2.2016.11.006

MEIJERS, A. J. S. (2014): The Southern Ocean in the coupled model intercomparison project phase 5. *Philosophical transactions. Series A, Mathematical, Physical, and Engineering Sciences*, A372: 20130296. doi: 10.1098/rsta.2013.0296

MENDES, C. R. B., TAVANO, V. M., DOTTO, T. S., KERR, R., DE SOUZA, M. S., GARCIA, C. A. E. and SECCHI, E. R. (2018): New insights on the dominance of cryptophytes in Antarctic coastal waters: A case study in Gerlache Strait. *Deep-Sea Research Part II: Topical Studies in Oceanography*, 149: 161–170. doi:10.1016/j.dsr2.2017.02.010

MENDES, C. R. B., TAVANO, V. M., LEAL, M. C., DE SOUZA, M. S., BROTAS, V. and GARCIA, C. A. E. (2013): Shifts in the dominance between diatoms and cryptophytes during three late summers in the Bransfield Strait (Antarctic Peninsula). *Polar Biology*, 36: 537-547. doi: 10.1007/s00300-012-1282-4

MEREDITH, M. P., KING, C. J. (2005): Rapid climate change in the ocean west of the Antarctic Peninsula during the second half of the 20th century. *Geophysical Research Letters*, 32: 1-5. doi: 10.1029/2005GL024042

MINICHEVA, H. G., ZOTOV, A. B. and KOSENKO, M. N. (2003): Methodical recommendations on the morpho-functional indexes define for unicellular and multicellular forms of aquatic vegetation. GEF UNDP Publication, 5-18.

MITCHELL, B. G., HOLM-HANSEN, O. (1991): Bio-optical properties of Antarctic Peninsula waters: Differentiation from temperate ocean models. *Deep Sea Research Part A. Oceanographic Research Papers*, 38: 1009-1028. doi: 10.1016/0198-0149(91)90094-V

MOLINE, M. A., CLAUSTRE, H., FRAZER, T. K., SCHOFIELD, O. and VERNET, M. (2004): Alteration of the food web along the Antarctic Peninsula in response to a regional warming trend. *Global Change Biology*, 10: 1973-1980. doi: 10.1111/j.1365- 2486.2004.00825.x

MONTES-HUGO, M., DONEY, S. C., DUCKLOW, H. W., FRASER, W. R., MARTINSON, D., STAMMERJOHN, S. E. and SCHOFIELD, O. (2009): Recent changes in phytoplankton communities associated with rapid regional climate change along the western Antarctic Peninsula. *Science*, 323: 1470-1473. doi: 10.1126/science.1164533

MONTES-HUGO, M., VEMET, M., MARTINSON, D. G., SMITH, R. and IANNUZZI, R. A. (2008): Variability on phytoplankton size structure in the Western Antarctic Peninsula (1997-2006). *Deep-Sea Research Part II: Topical Studies in Oceanography,* 55: 2106-2117.

NARDELLI, S. C., GRAY, P. C., STAMMERJOHN, S. E. and SCHOFIELD, O. (2023): Characterizing coastal phytoplankton seasonal succession patterns on the West Antarctic Peninsula. *Limnology and Oceanography*, 68(4): 845-861. doi: 10.1002/lno.12314

PRÉZELIN, B. B., HOFMANN, E. E., MENGELT, C. and KLINCK, J. M. (2000): The linkage between Upper Circumpolar Deep Water (UCDW) and phytoplankton assemblages on the West Antarctic Peninsula continental shelf. *Journal of Marine Research*, 58: 165-202. doi: 10.1357/002224000321511133

ROZEMA, P. D., VENABLES, H. J., VAN DE POLL, W. H., CLARKE, A., MEREDITH, M. P. and BUMA, A. G. J. (2017): Interannual variability in phytoplankton biomass and species composition in northern Marguerite Bay (West Antarctic Peninsula) is governed by both winter sea ice cover and summer stratification. *Limnology and Oceanography*, 62: 235-252. doi: 10.1002/lno.10391

SABA, G. K., FRASER, W. R., SABA, V. S., IANNUZZI, R. A., COLEMAN, K. E., DONEY, S. C., DUCKLOW, H. W., MARTINSON, D. G., MILES, T. N., PATTERSON-FRASER, D. L., STAMMERJOHN, S. E., STEINBERG, D. K. and SCHOFIELD, O. M. (2014): Winter and spring controls on the summer food web of the coastal West Antarctic Peninsula. *Nature Communications*, 5: 4318. doi: 10.1038/ncomms5318

SAILLEY, S. F., DUCKLOW, H. W., MOELLER, H. V., FRASER, W. R., SCHOFIELD, O. M., STEINBERG, D. K., GARZIO, L. M. and DONEY, S. C. (2013): Carbon fluxes and pelagic ecosystem dynamics near two western Antarctic Peninsula Adélie penguin colonies: An inverse model approach. *Marine Ecology Progress Series*, 492: 253-272. doi: 10.3354/meps10534

SCHOFIELD, O., SABA, G., COLEMAN, K., CARVALHO, F., COUTO, N., DUCKLOW, H., FINKEL, Z., IRWIN, A., KAHL, A., MILES, T., MONTES-HUGO, M., STAMMERJOHN, S. and WAITE, N. (2017): Decadal variability in coastal phytoplankton community composition in a changing West Antarctic Peninsula. *Deep Sea Research Part I: Oceanographic Research Papers*, 124: 42-54. doi: 10.1016/j.dsr.2017.04.014

SEREGIN, S. A., KUZMENKO, L. G., SYSOEV, A. A. and GAVRILOVA, N. A. (2005): Microplankton of the western part of Bransfield Strait: structure of abundance and biomass in the fall of 2002. *Morskiy ekologichnyi zhurnal*, 4(2): 68-81.

SERYOGIN, S. O., BRYANTSEVA, Y. V. and CHMIR, V. D. (2003): Microplankton (phyto- and bacterioplankton) during austral autumn in the coastal waters of the Argentina Islands Archipelago, Antarctica. *Ukrainian Antarctic Journal*, 1: 107-113. doi: 10.33275/1727-7485.1. 2003.632

SHERRELL, R. M., ANNETT, A. L., FITZSIMMONS, J. N., ROCCANOVA, V. J. and MEREDITH, M. P. (2018): A 'shallow bathtub ring' of local sedimentary iron input maintains the palmer deep biological hotspot on the West Antarctic Peninsula shelf. *Philosophical transactions. Series A,*

Mathematical, Physical, and Engineering Sciences, 376: 20170171. doi: 10.1098/rsta.2017.0171

STAMMERJOHN, S. E., MARTINSON, D. G., SMITH, R. C., YUAN, X. and RIND, D. (2008): Trends in Antarctic annual sea ice retreat and advance and their relation to El Niño–Southern Oscillation and Southern Annular Mode variability. *Journal of Geophysical Research: Oceans*, 113: C03S90. doi: 10.1029/2007JC004269

STAMMERJOHN, S., MASSOM, R., RIND, D. and MARTINSON, D. (2012): Regions of rapid sea ice change: An inter-hemispheric seasonal comparison. *Geophysical Research Letters*, 39: L06501. doi: 10.1029/2012GL050874

STEFELS, J., VAN LEEUWE, M. A., JONES, E. J., MEREDITH, M. P., VENABLES, H. J., WEBB, A. L. and HENLEY, S. F. (2018): Impact of sea-ice melt on DMS(P) inventories in surface waters of Marguerite Bay, West Antarctic Peninsula. *Philosophical Transactions of the Royal Society A: Mathematical, Physical and Engineering Sciences*, 376: 20170169. doi: 10.1098/rsta.2017.0169

STEINER, N., STEFELS, J. (2017): Commentary on the outputs and future of Biogeochemical Exchange Processes at Sea-Ice Interfaces (BEPSII). *Elementa: Science of the Anthropocene*, 5: 81. doi: 10.1525/ elementa.272

TURNER, J., COLWELL, S.R., MARSHALL, G.J., LACHLAN-COPE, T.A., CARLETON, A.M., JONES, P.D., LAGUN, V., REID, P.A. and IAGOVKINA, S. (2005): Antarctic climate change during the last 50 years. *International Journal of Climatology*, 25: 279-294. doi: 10. 1002/joc.1130

TURNER, J., LU, H., WHITE, I., KING, J. C., PHILLIPS, T., HOSKING, J. S., BRACEGIRDLE, T. J., MARSHALL, G. J., MULVANEY, R. and DEB, P. (2016): Absence of 21st century warming on Antarctic Peninsula consistent with natural variability. *Nature*, 535: 411-415. doi: 10.1038/ nature18645

VAN LEEUWE, M. A., FENTON, M., DAVEY, E., RINTALA, J. M., JONES, E. M., MEREDITH, M. P. and STEFELS, J. (2022): On the phenology and seeding potential of sea-ice microalgal species. *Elementa: Science of the Anthropocene*, 10(1): 00029. doi:10.1525/elementa.2021.00029

VAN LEEUWE, M. A., WEBB, A. L., VENABLES, H. J., VISSER, R. J. W., MEREDITH, M. P., ELZENGA, J. T. M. and STEFELS, J. (2020): Annual patterns in phytoplankton phenology in Antarctic coastal waters explained by environmental drivers. *Limnology and Oceanography*, 65: 1651-1668. doi: 10.1002/lno.11477

VARELA, M., FERNANDEZ, E. and SERRET, P. (2002): Size-fractionated phytoplankton biomass and primary production in the Gerlache and south Bransfield Straits (Antarctic Peninsula) in austral summer 1995–1996. *Deep-Sea Research Part II: Topical Studies in Oceanography*, 49: 749-768. doi: 10.1016/S0967-0645(01)00122-9

VENABLES, H. J., CLARKE, A. and MEREDITH, M. P. (2013): Wintertime controls on summer stratification and productivity at the western Antarctic Peninsula. *Limnology and Oceanography*, 58: 1035-1047. doi: 10.4319/lo.2013.58.3.1035

VERNET, M., MARTINSON, D., IANNUZZI, R., STAMMERJOHN, S., KOZLOWSKI, W., SINES, K., SMITH, R. and GARIBOTTI, I. (2008): Primary production within the sea-ice zone west of the Antarctic Peninsula: I – Sea ice, summer mixed layer, and irradiance. *Deep-Sea Research Part II: Topical Studies in Oceanography*, 55: 2068-2085. doi: 10.1016/j.dsr2.2008.05.021

VERNET, M., SMITH R. C. (2007): Measuring and modeling primary production in marine pelagic ecosystems. *In*: T. J. FAHEY and A. K. KNAPP (eds.): Principles and standards for measuring primary production. Oxford Univ. Press, pp. 142–174. doi: 10.1093/acprof:oso/9780195168662.001.0001

WEBB, A. L., VAN LEEUWE, M. A., DEN OS, D., MEREDITH, M. P., VENABLES, H. and STEFELS, J. (2019): Extreme spikes in DMS flux double estimates of biogenic sulfur export from the Antarctic coastal zone to the atmosphere. *Scientific Reports,* 9: 2233. doi: 10.1038/s41598-019-38714-4

ZOTOV, A. B. (2016): Possibilities of using phytoplankton surface indicators as phytoindicators of the EU Water Directive. *Hydrobiological Journal,* 2(52): 3-14. doi: 10.1615/HydrobJ.v52.i4.10

ZOTOV, A. B. (2008): The use of specific surface index in analyzing the morpho-structural organization of phytoplankton. *International Journal on Algae,* 10(4): 379-387. doi: 10.1615/ InterJAlgae.v10.i4.70

Supplementary Materials

The below-specified Tables are available and freely downloadable at the CPR web page (Vol. 14, No. 2, Zotov et al. 2024).

Table 1. Coordinates of phytoplankton monitoring stations in the waters of the Argentine Islands.

Table 2. Interannual differences in average abundance (N), biomass (B), surface area (S), surface index (ISC), average cell volume (V), specific surface (S/W), chlorophyll a concentration (Chl a) and pheophytin (Phae) of phytoplankton groups in the waters of the Argentine Islands in the late summer period of 2019-2021 (Multiple Range Tests for 95.0% LSD).

Table 3. Distribution of phytoplankton abundance ($10^6 \cdot m^{-3}$) between taxonomic classes in the Argentine Islands waters in late summer period 2019-2021.

Table 4. Distribution of phytoplankton biomass ($mg \cdot m^{-3}$) between taxonomic classes in the Argentine Islands waters in late summer period 2019-2021.

Table 5. Distribution of phytoplankton surface area ($mkm^2 \cdot m^{-3}$) between taxonomic classes in the Argentine Islands waters in late summer period 2019-2021.

Table 6. Averages and standard deviations for abundance (N, $10^6 \cdot m^{-3}$), biomass (B, $mg \cdot m^{-3}$), surface area (S, $\mu m^2 \cdot m^{-3}$), surface index (ISC, m^{-1}), specific surface (S/W, $m^2 \cdot kg^{-1}$) and average cells' volume (V, mkm^3) of phytoplankton in the Argentine Islands waters in 2019-2021.

Table 7. Monthly averages and standard deviations for abundance (N, $10^6 \cdot m^{-3}$), biomass (B, $mg \cdot m^{-3}$), surface area (S, $\mu m^2 \cdot m^{-3}$), surface index (ISC, m^{-1}), specific surface (S/W, $m^2 \cdot kg^{-1}$) and average cells' volume (V, mkm^3) of phytoplankton in the Argentine Islands waters in 2020-2021.